Functional Deficits in Autistic Disorder: Characterization by Technetium-99m-HMPAO and SPECT

James M. Mountz, Lelland C. Tolbert, Duncan W. Lill, Charles R. Katholi and Hong-Gang Liu

Division of Nuclear Medicine, Department of Radiology, and Departments of Psychiatry and Biostatistics, University of Alabama Medical Center, Birmingham, Alabama

Autistic disorder is an early and severe developmental disorder characterized by deficits in verbal and nonverbal language, social skills, cognitive functioning and an abnormal repertoire of behaviors. Current research, however, has failed to identify the neurobiological mechanisms that underlie autism or those cortical brain regions, if any, that are abnormal. **Methods:** We examined regional cerebral blood flow (rCBF) in six young, severely autistic patients. High-resolution brain SPECT with ^{99m}Tc-HMPAO was performed while five of the six patients were under general anesthesia. The scans reflected the subjects' rCBF in their usual alert behavioral state, since the tracer was injected at least 15 min prior to anesthesia and is rapidly extracted and fixed in the brain. A computer-automated cortical region of interest (ROI) generator was used to define 12 annular cortical regions (region 1 = left frontal, clockwise to region 12 = right frontal) for count data acquisition. The ratio of average counts in each ROI to whole-slice counts for the autistic patients was compared to age-matched controls using repeated measures (split-plot) ANOVA statistical analysis for three representative brain levels. **Results:** In the autistic patients, cortical regions 3, 4, and 10 were abnormally low at the cortical level canthomeatal (CM) + 3.5 cm. At level CM + 5.5 cm, regions 3, 4, 5 and 10 were abnormally low, and at level CM + 7.5 cm, regions 7 and 9 were also abnormally low. These regions correspond to abnormally low rCBF values located predominately in the temporal and parietal lobes, with the left cerebral hemisphere showing greater rCBF abnormalities than the right. **Conclusion:** Our findings suggest that the temporal and parietal lobes have abnormal rCBF in autism. HMPAO brain SPECT in combination with general anesthesia is particularly useful for imaging severely noncompliant patients.

Key Words: autism; technetium-99m-HMPAO; regional cerebral blood flow; single-photon emission computed tomography

J Nucl Med 1995; 36:1156–1162

Autism is an early and severe developmental disorder characterized by deficits in verbal and nonverbal language, social skills, cognitive functioning and an abnormal repertoire of behaviors as defined by DSM-III-R criteria (*1*). Little is known about the neurobiological mechanisms that underlie this disorder. Huebner (*2*) supports the notion that autism should be viewed as an expression of an undefined neurologic disorder. Current research shows that a spectrum of neurological abnormalities involving the brainstem, cerebellum, midbrain, frontal lobe and possible other brain regions may be present in autism. Gillberg (*3*) reported that genetic factors play a role in autism and that it might best be perceived as a behavioral syndrome reflecting underlying brain dysfunction which "shades into other clinical syndromes." The heterogeneous symptomatology found in autism has led many to believe that attempts to determine an underlying cause may be futile (*3*).

A variety of imaging techniques have been used to study autism in an attempt to localize the region(s), of the brain responsible for its heterogeneous symptomatology. Several investigators have used MRI to examine brain structures (*4–8*), but no consistent abnormalities in either the supratentorial or cerebellar regions were not found. Fluorine-18-fluorodeoxyglucose PET (FDG-PET) has been used to measure the regional metabolic rate of glucose utilization in the brain of autistic subjects, but the abnormalities were heterogeneous (*9–10*). A ^{133}Xe SPECT study (*11*) did not show any abnormal brain regional cerebral blood flow (rCBF).

The majority of the imaging studies on autism have found no abnormality in rCBF. Of those studies in which an abnormality was identified, the abnormality resided solely within the cerebellum or the brainstem. Courchesne et al. performed a single MRI study of the brain which showed parietal lobe abnormalities in autistic disorder (*12*). George et al. also found rCBF abnormalities involving the frontal and temporal lobes in a ^{99m}Tc-HMPAO SPECT study of four autistic adults who were not sedated (*13*).

Abnormal temporal lobe function possibly plays a role in the pathogenesis of autism (*14*), since normal functioning of the amygdala and hippocampus is crucial to the regulation and integration of affect, memory and learning (*15*).

Received Jul. 28, 1994; revision accepted Mar. 7, 1995.

For correspondence or reprints contact: James M. Mountz, MD, PhD, Division of Nuclear Medicine, University of Alabama Hospital, 619—19th Street South, Birmingham, AL 35233.

Consequently, dysfunction of these temporal lobe structures have been implicated in the etiopathology of autism.

Since abnormalities in temporal lobe function have been implicated in autistic disorder, we hypothesize that rCBF abnormalities should be evident in the cortical structures, including, but not necessarily limited to, the temporal lobe. Therefore, we studied six young severely autistic subjects to evaluate rCBF findings from the frontal, temporal, occipital and parietal cortical regions, and the caudate and thalamus.

PATIENTS AND METHODS

Autistic subjects were selected on a volunteer basis from the Glenwood Mental Health Services Inc., Birmingham, AL. The study population consisted of 1 girl and 5 boys (average age, 13.7 yr; range 9 to 21 yr). Informed consent was obtained from the legal guardian for all subjects prior to study participation. The study protocol was approved by the University of Alabama at Birmingham Medical Center Institutional Review Board. All six subjects satisfied DSM-III-R criteria for autistic disorder and were evaluated and scored by the autistic symptom inventory educational profile (ASIEP) (*16*) in accordance with items from the autistic behavior checklist (ABC) scale.

Subject 1, a 9-yr-old boy, had a performance IQ of 45 and an ABC score of 85. Subject 2, a 10-yr-old boy, had a performance IQ of 32 and an ABC score of 90. Subject 3, a 13-yr-old girl, had a performance IQ of 51 and an ABC score of 66. Subject 4, a 14-yr-old boy, had a performance IQ of 70 and an ABC score of 80. Subject 5, a 15-yr-old boy, had a performance IQ of 72 and an ABC score of 71. Subject 6, a 21-yr-old man, had a performance IQ of 100 and an ABC score of 85.

For ethical reasons, radioactive tracer could not be injected into normal children. The control group consisted of two girls and five boys, (mean age, 13.1 yr; range, 6 to 20 yr). Five were selected from 14 children who had ^{99m}Tc-HMPAO brain SPECT studies at our institution between 1990 to 1994 for a suspected neurologic problem which was found to be due to another cause retrospectively. The remaining control group subjects were normal volunteers (two men, aged 18 and 20 yr). All ^{99m}Tc-HMPAO SPECT scans as well as the MRI and CT scans were interpreted as normal. No control group subject had prior or subsequent history of neurologic disease. The control group subjects who had previous HMPAO brain SPECT imaging had recovered from their illness completely for which SPECT scanning had been performed. No difference in rCBF values were found between the two normal and the five other controls. The rCBF data for the autistic group were compared to the rCBF values of the control group.

Brain SPECT Imaging

Technetium-99m-HMPAO was administered intravenously. The patients were allowed to regain composure after the needle insertion at which time the standard adult dose (for 70 kg weight) of 740 MBq (20 mCi) adjusted for age by the formula:

$$[(\text{age} + 1)/(\text{age} + 7)] \times [(\text{standard adult dose})],$$

was injected through the intravenous line. During this injection phase, the patients were in their usual state of behavior in a dimly lit room with minimal ambient sound. The patients remained in this condition for 15 min and were then taken to the nuclear medicine imaging suite where general anesthesia was administered (approximately 0.15 mg/kg medazolam and 10 mg/kg ketamine). General anesthesia was required for acquisition of tomographic data in five of the six autistic subjects because they were severely low-functioning and were unable to remain still for the duration of the scan. Patient 6 did not require general anesthesia.

HMPAO achieves a fixed uptake pattern in the brain within 10 min after intravenous administration (*17*). Thus, although SPECT scanning was performed after induction of general anesthesia, radiotracer distribution in the brain reflected rCBF at the time the subject was injected with ^{99m}Tc-HMPAO. The scans were acquired on a dual-head gamma camera equipped with a high-resolution collimator, which yielded an image resolution of approximately 8.5 mm FWHM. While under general anesthesia, Patients 2 and 4 underwent CT scanning. Three patients had MR scanning using a standardized reference system (*18,19*) which enabled accurate alignment of the SPECT scan to the anatomic scan for identification of anatomic regions of interest (ROIs).

Brain SPECT Image Analysis

Reconstruction of the scan data yielded transverse sections aligned parallel to and sequentially above the canthomeatal (CM) line as determined by a reference system method (*20–22*). The accuracy of structural correlation between SPECT to CT or MRI has been previously described (*19,22*). A computer-automated cortical annulus was defined on the transverse rCBF brain SPECT images by generating an outer boundary at the 50% counts per pixel value of the mean counts per pixel in the section being analyzed. An inner boundary was defined by a border positioned 15.68 mm (8 pixels) radially inward from the outer border (*21,22*). Figure 1 illustrates, on a lateral brain diagram, the location of the three selected brain sections from which image data were obtained. Also shown in Figure 1 are the approximate locations of the major lobes of the brain in relation to the individual cortical regions of this annulus. ROIs corresponding to the caudate nucleus and thalamus were delineated by localizing these structures

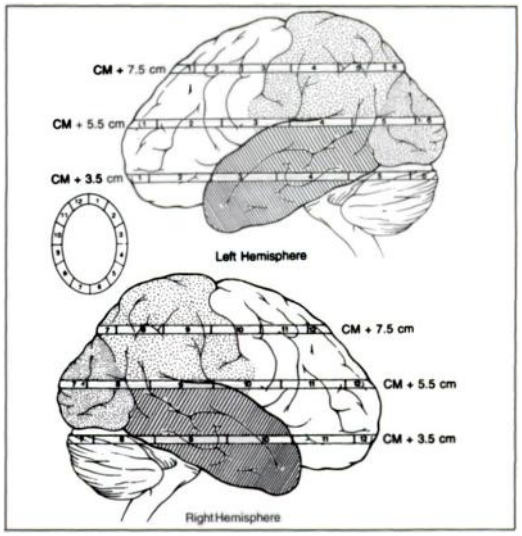

FIGURE 1. Individual cortical ROIs created by subdividing the cortical annulus into equal angular sectors approximately corresponding to brain lobar structures as shown. Regions 1, 2, 11 and 12 are CM + 3.5 cm = inferior frontal. Regions 3 and 10 are CM + 3.5 cm = anterior temporal. Regions 4 and 9 are CM + 3.5 cm = posterior temporal. Regions 6 and 7 are CM + 5.5 cm = occipital. Regions 1, 2, 11 and 12 are CM + 7.5 cm = superior frontal. Regions 4, 5, 8 and 9 are CM + 7.5 cm = midparietal.

on the SPECT scan from the CT or MRI scan using anatomic SPECT coregistered images by a method perfected at our institution (*19,22*). The anatomically delineated ROIs were directly translated from the anatomic to the SPECT image using the reference system and the coregistration image superimposition method (*19,22*). ROI boundaries on the SPECT images for these subcortical structures corresponded to the structure boundary directly visualized on the CT or MR image.

Average counts per pixel from each region were used for analysis. SPECT image data from the age-matched controls were obtained with the same protocol used for the autistic subjects, and average counts per pixel were obtained for analysis. Normalization of regional count data was performed by dividing the average counts per pixel by the average counts per pixel in the section under analysis (defined as the average counts within the outer boundary of the whole slice annulus) (*20,21,23*). Regional analysis was performed by comparing between group rCBF for each cortical region as well as for both the caudate nuclei and hemithalami. Statistical analysis was performed using a split-plot (repeated measures) analysis of variance (ANOVA) model.

RESULTS

SPECT Resolution

Technetium-99m-HMPAO brain SPECT image resolution was excellent at the cortex (approximately 8.5 mm FWHM) in all six autistic subjects. This excellent resolution was due to the relative small radius of rotation and lack of head motion since five of the patients were anesthetized during imaging.

SPECT, CT and MRI

All six patients had normal CT or MR scans. Figure 2A shows sections from the ^{99m}Tc-HMPAO brain SPECT scan for Patient 2, illustrating low and asymmetric tracer uptake in the inferior frontal, anterior temporal, posterior temporal, occipital, cerebellum and caudate nucleus brain regions. Figure 2B shows corresponding sections from the normal CT scan for this same subject. Both scans were obtained while the patient was anesthetized.

Figure 3A shows six sequential ^{99m}Tc-HMPAO brain SPECT scan sections from Patient 1, demonstrating low and asymmetric tracer uptake in the right midparietal and posterior frontal lobes. Figure 3B shows coregistered brain sections, illustrating the MR, SPECT and the fusion image for the same subject. These sections are at the CM + 7.5 cm level and show asymmetric and low tracer uptake by the right posterior frontal lobe and the entire right parietal lobe.

Figure 4A shows eight sequential ^{99m}Tc-HMPAO SPECT scan sections from Patient 4, which demonstrate low tracer uptake in the posterior temporal and occipital brain regions. Figure 4B shows coregistered brain sections illustrating the MR, ^{99m}Tc-HMPAO brain SPECT and fusion image for this same patient. These sections are at the level of the temporal and occipital lobes and show markedly reduced tracer uptake in the posterior temporal and occipital lobes. The MR scan was normal, and the gyral prominence on the T1-weighted image is purposely enhanced (by image thresholding) so that the gyri can be seen

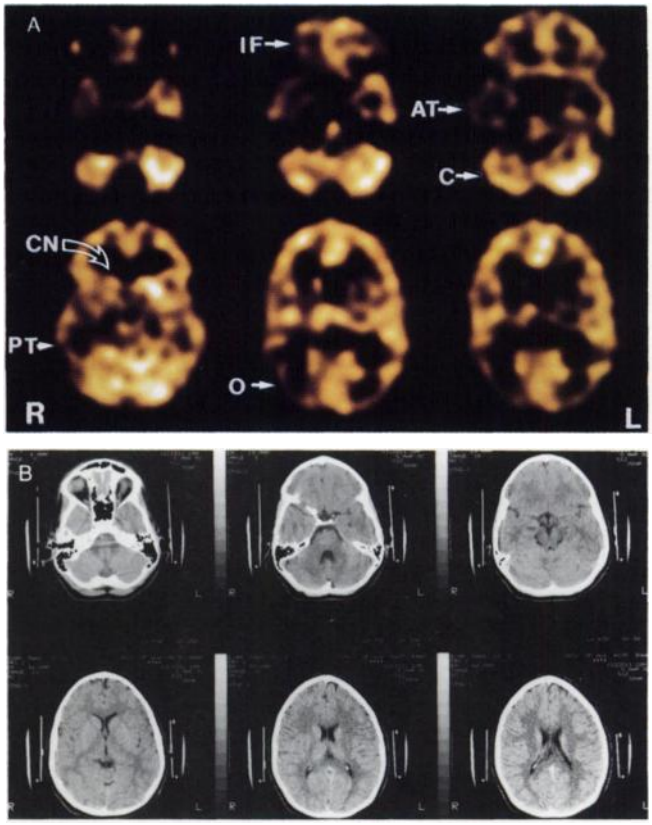

FIGURE 2. (A) Abnormal ^{99m}Tc-HMPAO brain SPECT scan of Patient 2 shows asymmetric and low tracer uptake by the right inferior frontal region (IF), the inferior and superior anterior temporal regions (AT), the right cerebellar hemisphere (C), the right caudate nucleus (CN), the posterior temporal region (PT) and the right occipital lobe (O). (B) Normal CT scan of Patient 2. The six CT sections are at the same orientation and level as the corresponding SPECT slices.

on the fusion image. The same degree of gyri prominence is seen both frontally and in the posterior temporal regions, indicating that a focal atrophic process is unlikely to account for the extensive diminution of tracer uptake in the posterior temporal lobes. The SPECT scan findings for this subject emphasize the dominant involvement of the temporal lobes. Figure 5 illustrates the average rCBF values for all autistic patients compared with controls for each cortical level and illustrates temporal lobe abnormalities at CM + 3.5 cm and CM + 5.5 cm and parietal abnormalities at CM + 7.5 cm.

Data Analysis

Data were analyzed using a split-plot (repeated measures) ANOVA model at each brain section level. The two groups were the whole plots, while the regions were the corresponding subplots (repeated measures). The autistic subjects were compared to the control subjects. The results of the regional analysis comparing the average value in each ROI to the total count within a circumferential ROI around the entire cortical slice under analysis show that at level CM + 3.5 cm there is no significant interaction effect ($p > 0.34$), meaning that the responses of the two groups

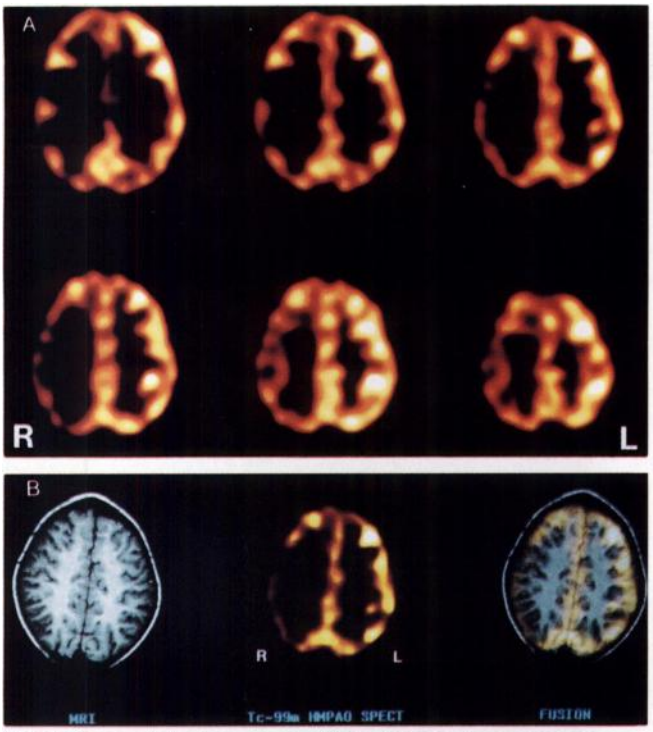

FIGURE 3. (A) Six sequential ^{99m}Tc-HMPAO brain SPECT scan sections from Patient 1 show low and asymmetric right parietal and right posterior frontal tracer uptake (CM + 7.5 cm; regions 7–11). (B) Coregistered MR, SPECT and fusion image at section level CM + 7.5 cm. The MRI section (left) is normal. The coregistered ^{99m}Tc-HMPAO brain SPECT scan section (middle) shows low and asymmetric tracer uptake by the parietal and posterior frontal lobes, right lower than left, with no corresponding anatomic abnormality, as demonstrated by the MRI-SPECT fusion image (right).

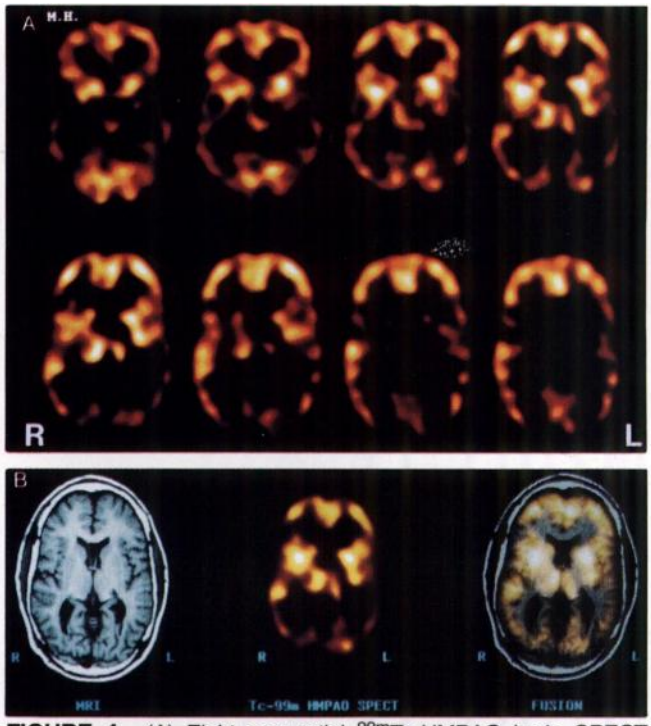

FIGURE 4. (A) Eight sequential ^{99m}Tc-HMPAO brain SPECT sections from Patient 4 show low tracer uptake by the posterior temporal and occipital lobes (CM + 5.5 cm, regions 4–8) and (CM + 7.5 cm, regions 3–9), respectively. (B) Coregistered MR, SPECT and fusion image at the level of the temporal and occipital lobes. The MRI section (left) is normal. The coregistered ^{99m}Tc-HMPAO brain SPECT section (middle) shows bilateral posterior temporal (left lower than right) and bilateral occipital diminution of tracer uptake with no corresponding anatomic abnormality, as demonstrated by the MRI-SPECT fusion image (right).

are parallel. There is a highly significant overall group effect ($p < 0.0009$), indicating parallel regional profiles rather than identical profiles. There are also highly significant regional effects ($p < 0.001$). Multiple comparisons of the means of each region yielded the following significant probability values (regions 3, 4, 10): 0.0064, 0.0223 and 0.0093. The other regions at this level failed to reject ($p > 0.12$).

At level CM + 5.5 cm, the results of multiple comparison showed the following significant differences (region 3, 4, 5, 10): probability values were 0.0011, 0.0047, 0.0089 and 0.0011. At level CM + 7.5 cm, the results of multiple comparison showed the following significant differences (regions 7, 9): probability values are 0.0142 and 0.0127. A comparison of the caudate nuclei and thalami showed significant reduced rCBF to the right caudate nucleus ($p < 0.02$).

Table 1 summarizes the results of the probability values for each cortical region. Bilateral and statistically significant temporal lobe reductions in rCBF are evident at regions 3, 4, and 10, all having significant probability values at level CM + 3.5 cm (Table 1, Fig. 5). Left cerebral lateralization of the rCBF defect is indicated by a greater number of significant probability values and lower rCBF values in regions 3 to 5 at CM + 3.5 cm and CM + 5.5 cm. Bilateral parietal lobe reductions in rCBF is evident at regions 4 to 10 at CM + 7.5 cm (Fig. 5). There are slightly worse reductions of rCBF to the right parietal lobe as indicated by the lower probability values in regions 7 and 9 at CM + 7.5 cm (Table 1). Table 2 summarizes the results obtained from statistical analysis.

DISCUSSION

Structural Imaging

MRI studies of subjects with autism have varied and sometimes have had conflicting results. In a series of reports, Courchesne et al. (*24–27*) noted evidence for cerebellar abnormalities, particularly those involving lobules VI and VII. Replication of these reports has been problematic, and several groups (*28–30*) have contradicted these reports. Similarly, another MRI study of 29 autistic children found that the midbrain and pons were significantly smaller, suggesting that brainstem structure was anatomically altered in autistic children (*31*). This study conflicted with a MRI study in which the size of the entire pons and several regions within the brainstem were the same in the autistic and control subjects (*32*).

Several MRI studies have implicated supratentorial abnormalities in autism. Piven et al. reported on five autistic

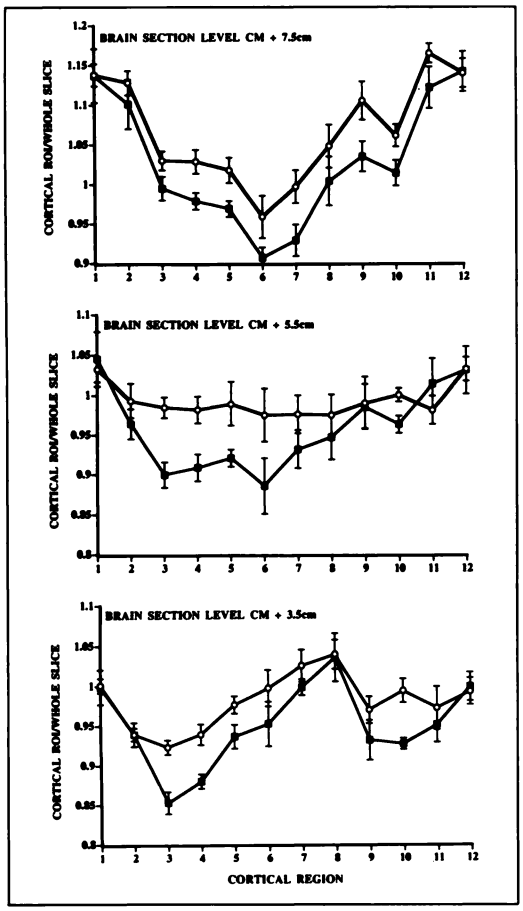

FIGURE 5. (Top) Average rCBF values for the autistic (solid box) and control groups (open circles) at cortical level CM + 7.5 cm. (Middle) Average rCBF values for the autistic (solid box) and control groups (open circles) at cortical level CM + 5.5 cm. (Bottom) Average rCBF values for the autistic (solid box) and control groups (open circles) at cortical level CM + 3.5 cm. Error bars are ± s.e.m.

TABLE 1
Probability Values for Individual Cortical Regions

Region	CM + 3.5 cm*	CM + 5.5 cm†	CM + 7.5 cm‡
1			
2			
3	0.0064	0.0011	
4	0.0223	0.0047	0.0765
5		0.0089	0.0626
6	0.0798		
7		0.0872	0.0142
8			
9		0.0591	0.0127
10	0.0093	0.0011	0.0886
11			
12			

*Probability values on all tests which failed to show significance were $p > 0.12$.
†Probability values on all tests which failed to show significance were $p > 0.22$.
‡Probability values on all tests which failed to show significance were $p > 0.11$.

patients with polymicrogyria, one with schizencephaly and macrogyria and one with macroglia (*33*). Hashimoto et al. compared 18 autistic patients with 11 mentally retarded patients and 18 controls and found altered left-to-right ratios in the frontal lobe volume of the autistic and retarded subjects. The asymmetry was more severe in the autistic subjects (*34*). The most salient point is made by Nowell et al. (*28*). In their study, MRI revealed 53 autistic patients with normal midsagittal vermian height and shape measurements, normal anterior/posterior brain size and normal ventricular dimension and size. In summary, these studies illustrate that MRI findings in autistic patients are highly variable.

Temporal Lobe Abnormalities

Temporal lobe abnormality in autistic disorder was cited in a case report of a healthy man who contracted herpes encephalitis at age 31 yr (*35*) and developed all the symptoms considered diagnostic of autism. This report cast doubt on the notion that autism results exclusively from a developmental disorder and suggests that temporal lobe damage may cause autism in certain cases. Hoon and Reiss (*36*) investigated human and nonhuman primate pathological processing affecting the temporal lobe and noted that abnormalities in these brain regions are related to development of autistic syndrome. They reported a case of a young boy with left temporal oligodendroglioma who demonstrated a constellation of autistic behaviors meeting DSM-III-R criteria for pervasive developmental disorders. Abnormalities in social interaction and affective expression in communication were particularly evident, and while some of the symptoms improved after tumor resection, other signs of qualitative abnormalities in development emerged and persisted. These facts support the hypothesis that damage to temporal lobe structures during an early developmental period may result in autistic disorder.

Functional Imaging

Functional imaging is a more sensitive technique for detecting brain dysfunction. Therefore, several investigators have used PET and SPECT to study autism. Initial functional imaging studies by PET and SPECT were not helpful, however, in localizing a characteristic abnormality in autism. Influenced by reports that autistic patients may have fewer Purkinje and granule cells, Heh et al. found no significant difference in mean cerebellar vermis glucose metabolism between autistic subjects and normal controls (*37*). Herold et al. found no differences in rCBF, oxygen consumption and glucose consumption in a PET study of six autistic patients (*38*). DeVolder et al. also failed to find abnormal glucose metabolism in a PET study of autism; however, this study was performed on relatively highly functioning individuals after sedation.

In a ^{133}Xe SPECT study of autism, Zibovicious also failed to detect rCBF abnormalities, but their patients were sedated with phenobarbital and droperidol, which are known to alter rCBF. George et al. studied four autistic

TABLE 2
Errors and Probabilities Found in Split-Plot ANOVA Statistical Data Analysis for Each Cortical Level

Source	df	Mean square	F value	p > F
Level CM + 3.5 cm				
Group	1	0.03633448	20.14	0.0009
Error (Group)	11	0.00180423		
Region	11	0.02254620	10.80	0.0001
Group by region	11	0.00234837	1.12	0.3480
Error	121	0.00208789		
Level CM + 5.5 cm				
Group	1	0.06895800	4.23	0.0643
Error (Group)	11	0.01631579		
Region	11	0.01616326	7.70	0.0001
Group by region	11	0.00535977	2.55	0.0061
Error	121	0.00209866		
Level CM + 7.5 cm				
Group	1	0.02546807	14.49	0.0029
Error (Group)	11	0.00440091		
Region	11	0.06689271	27.02	0.0001
Group by region	11	0.00162933	0.66	0.6172
Error	121	0.00247533		

adults using ^{99m}Tc-HMPAO (*13*). Their results were similar to ours in that autistic subjects had decreased rCBF in the temporal and frontal lobes in comparison to the controls. We also found decreases in frontal rCBF in our autistic group (Fig. 5), but this was not statistically significant. Our temporal lobe findings are statistically significant, however, and indicate predominant involvement of this region in autism.

CONCLUSION

Functional studies with FDG-PET and ^{133}Xe SPECT may have failed to detect neurologic abnormalities due to sedation effects or because study subjects were relatively highly functional and could comply with the imaging protocol: namely, to lie still without sedation.

George et al. (*13*) studied autistic adults who could lie still and rCBF abnormalities were detected. Our study extends the results of George et al. to an adolescent population and supports the presence of a functional abnormality in the cerebral cortex that predominately involves the temporal and parietal lobes. This finding is consistent with our hypothesis and that of other investigators (i.e., that an abnormality of the temporal lobe (or lobes) is present in autism. Furthermore, our study demonstrates the advantages of using sedation with ^{99m}Tc-HMPAO brain SPECT in severely noncompliant subjects by capitalizing on the nonredistributive property of ^{99m}Tc-HMPAO.

These results are preliminary and speculation on the outcome of these findings on future therapies for autism is premature. Since the anatomic scans were normal, the early detection of these abnormalities by functional imaging may provide the best method to obtain information necessary to quantify the potential benefit of ongoing therapeutic methods and possibly evaluate new therapies.

ACKNOWLEDGMENTS

The authors thank Ms. Dorothea Ballard for administrative assistance and Dr. Fiona Hunter for editorial assistance in the preparation of this manuscript. We are indebted to the cooperation of Dr. Thomas Vaughan and the Glenwood Mental Health Services Inc. for their assistance. This work was supported in part by a Student Fellowship from the Education and Research Foundation of the Society of Nuclear Medicine (DWL); a grant from the Civitan International Research Center, Birmingham, AL (LCT); and grant 1R01 HD32100-01 from the National Institute of Child Health and Human Development (JMM).

REFERENCES

1. American Psychiatric Association. *Diagnostic and statistical manual of mental disorders.* Third edition—revised (DSM-III-R). Washington, DC: American Psychiatric Association; 1987.
2. Huebner RA. Autistic disorder: a neuropsychological enigma. *Am J Occup Ther* 1992;46:487–501.
3. Gillberg CL. Autism and autistic-like conditions: subclasses among disorders of empathy. *J Child Psychol Psychiatry* 1992;33:813–842.
4. Gaffney GR, Tsai LY, Kuperman S, Minchin S. Cerebellar structure in autism. *Am J Dis Child* 1987;141:1330–1332.
5. Gaffney GR, Kuperman S, Tsai LY, Minchin S, Hassanein KM. Midsagittal magnetic resonance imaging of autism. *Br J Psychiatry* 1987;151:831–833.
6. Ekman G, DeChateau P, Marions O, Sellden H, Wahlund LO, Wetterberg L. Low field magnetic resonance imaging of the central nervous system in 15 children with autistic disorder. *Acta Paediatr Scand* 1991;80:243–247.
7. Garber HJ, Ritvo ER. Magnetic resonance imaging of the posterior fossa in autistic adults. *Am J Psychiatry* 1992;148:245–247.
8. Kjos BO, Umansky R, Barkovich AJ. Brain MR imaging in children with developmental retardation of unknown cause: results in 76 cases. *Am J Neuroradiol* 1990;11:1035–1040.
9. Siegel BV, Asarnow R, Tanguay P, et al. Regional cerebral glucose metabolism and attention in adults with a history of childhood autism. *J Neuropsych Clin Neurosci* 1992;4:406–414.
10. Buchsbaum MS, Siegel BV, Wu JC, Hazlett E, Sicotte N, Haier R. Brief report: attention performance in autism and regional brain metabolic rate assessed by positron emission tomography. *J Autism Devel Dis* 1992;22: 115–125.
11. Zilbovicius M, Garreau B, Tzourio N, et al. Regional cerebral blood flow in childhood autism: a SPECT study. *Am J Psychiatry* 1992;149:924–930.
12. Courchesne E, Press GA, Yeung-Courchesne R. Parietal lobe abnormalities detected with MR in patients with infantile autism. *AJR* 1993;160:387–393.
13. George MS, Costa DC, Kouris K, Ring HA, Ell PJ. Cerebral blood flow abnormalities in adults with infantile autism. *J Nerv Ment Dis* 1992;180:413–417.
14. Damasio AR, Maurer RG. A neurological model for childhood autism. *Arch Neurol* 1978;35:777–786.
15. Mesulam M. Patterns in behavioral neuroanatomy: association areas, the limbic system and hemispheric specialization. In: *Principles of behavioral neurology.* Philadelphia: FA Davis; 1985:37/40.
16. Krug DA, Arick JR, Almond PJ. Behavior checklist for identifying severely handicapped individuals with high levels of autistic behavior. *J Child Psychol Psychiatry* 1980;21:221–229.
17. Andersen AR, Friberg H, Lassen NA, Kristensen K, Neirinckx RD. Serial studies of cerebral blood flow using ^{99m}Tc-HMPAO: a comparison with ^{133}Xe. *Nucl Med Commun* 1987;8:549–557.
18. Wilson MW, Mountz JM. A reference system for neuroanatomical local-

ization on functional reconstructed cerebral images. *J Comput Assist Tomogr* 1989;174–178.
19. Mountz JM, Wilson MW, Wolff CG, Deutsch G, Harris JM. Validation of a reference method for correlation of anatomic and functional brain images. *Computerized Medical Imaging and Graphics* 1994;18:163–174.
20. Mountz JM, Deutsch G, Khan SH. An atlas of regional cerebral blood flow changes in stroke imaged by ^{99m}Tc-HMPAO SPECT with corresponding anatomic image comparison. *Clin Nucl Med* 1993;18:1067–1082.
21. Mountz JM, Deutsch G, Kuzniecky R, Rosenfeld SS. Brain SPECT: 1994 update. In: Freeman LM, ed. *Nuclear medicine annual*. New York: Raven Press; 1994:1–54.
22. Mountz JM, Zhang B, Liu HG, Inampudi C. A reference method for correlation of anatomic and functional brain images: validation and clinical application. *Semin Nucl Med* 1994;XXIV:256–271.
23. Mountz JM. Quantification of the SPECT brain scan. In: Freeman LM, ed. *Nuclear Medicine Annual.* New York: Raven Press; 1991:67–98.
24. Murakami JW, Courchesne E, Press GA, Yeung-Courchesne R, Hesselink JR. Reduced cerebellar hemisphere size and its relationship to vermal hypoplasia in autism. *Arch Neurol* 1989;46:689–694.
25. Courchesne E. Neuroanatomic imaging in autism. *Pediatrics* 1991;87:781–790.
26. Courchesne E, Hesselink JR, Jernigan TL, Yeung-Courchesne R. Abnormal neuroanatomy in a nonretarded person with autism. Unusual findings with magnetic resonance imaging. *Arch Neurol* 1987;44:335–341.
27. Yeung-Courchesne R, Courchesne E, Saitoh O, Townsend JP. Hyperplasia as well as hypoplasia of vermal lobules VI-VII in patients with autism. *Proc Soc Neurosci* 1993;19:183.
28. Nowell MA, Hackney DB, Muraki AS, Coleman M. Varied MR appearance of autism: 53 pediatric patients having the full autistic syndrome. *Magn Reson Imaging* 1990;8:811–816.
29. Kleiman MD, Neff S, Rossman NP. The brain in infantile autism: are posterior fossa structures abnormal? *Neurology* 1992;42:753–760.
30. Piven J, Nehme E, Simon J, Barta P, Pearlson G, Folstein SE. Magnetic resonance imaging in autism: measurement of the cerebellum, pons and fourth ventricle. *Biol Psychiatry* 1992;31:491–504.
31. Hashimoto T, Tayama M, Miyazaki M, et al. Reduced midbrain and pons size in children with autism. *Tokusima J Exp Med* 1991;38:15–18.
32. Hsu M, Yeunge-Courchesne R, Courchesne E, Press GA. Absence of magnetic resonance imaging evidence of pontine abnormality in infantile autism. *Arch Neurol* 1991;48:1160–1163.
33. Piven J, Berthier ML, Starkstein SE, Nehme E, Pearlson G, Folstein S. Magnetic resonance imaging evidence for a defect of cerebral cortical development in autism. *Am J Psychiatry* 1990;147:734–739.
34. Hashimoto T, Tayama M, Mori K, Fujino K, Miyazaki M, Kuroda Y. Magnetic resonance imaging in autism: preliminary report. *Neuropediatrics* 1989;20:142–146.
35. Gillberg IC. Autistic syndrome with onset at age 31 years: herpes encephalitis as a possible model for childhood autism. *Dev Med Child Neurol* 1991;33:920–924.
36. Hoon AH Jr, Reiss AL. The mesial-temporal lobe and autism: case report and review. *Dev Med Child Neurol* 1992;34:252–259.
37. Heh CW, Smith R, Wu J, et al. Positron emission tomography of the cerebellum in autism. *Am J Psychiatry* 1989;146:242–245.
38. Herold S, Frackowiak RS, LeCouteur A, Rutter M, Howlin P. Cerebral blood flow and metabolism of oxygen and glucose in young autistic adults. *Psychol Med* 1988;18:823–831.
39. DeVolder A, Bol A, Michel C, Congneau M, Goffinet AM. Brain glucose metabolism in children with the autistic syndrome: positron tomography analysis. *Brain Dev* 1987;9:581–587.